2023. 19(1). 64–72

СТРОИТЕЛЬНАЯ МЕХАНИКА ИНЖЕНЕРНЫХ КОНСТРУКЦИЙ И СООРУЖЕНИЙ

STRUCTURAL MECHANICS OF ENGINEERING CONSTRUCTIONS AND BUILDINGS

ISSN 1815-5235 (Print), 2587-8700 (Online)

HTTP://JOURNALS.RUDN.RU/STRUCTURAL-MECHANICS

DOI 10.22363/1815-5235-2023-19-1-64-72
EDN: FVOZAA
UDC 539.3

RESEARCH ARTICLE / НАУЧНАЯ СТАТЬЯ

Quadrilateral element in mixed FEM for analysis of thin shells of revolution

Yuriy V. Klochkov[1], Valeria A. Pshenichkina[2], Anatoliy P. Nikolaev[1], Olga V. Vakhnina[1], Mikhail Yu. Klochkov[2]

[1] *Volgograd State Agrarian University, Volgograd, Russian Federation*
[2] *Volgograd State Technical University, Volgograd, Russian Federation*
klotchkov@bk.ru

Article history
Received: November 15, 2022
Revised: February 20, 2023
Accepted: February 24, 2023

For citation
Klochkov Yu.V., Pshenichkina V.A., Nikolaev A.P., Vakhnina O.V., Klochkov M.Yu. Quadrilateral element in mixed FEM for analysis of thin shells of revolution. *Structural Mechanics of Engineering Constructions and Buildings.* 2023;19(1):64–72. http://doi.org/10.22363/1815-5235-2023-19-1-64-72

Abstract. The purpose of study is to develop an algorithm for the analysis of thin shells of revolution based on the hybrid formulation of finite element method in two dimensions using a quadrilateral fragment of the middle surface as a discretization element. Nodal axial forces and moments, as well as components of the nodal displacement vector were selected as unknown variables. The number of unknowns in each node of the four-node discretization element reaches nine: six force variables and three kinematic variables. To obtain the flexibility matrix and the nodal forces vector, a modified Reissner functional was used, in which the total specific work of stresses is represented by the specific work of membrane forces and bending moments of the middle surface on its membrane and bending strains, and the specific additional work is determined by the specific work of membrane forces and bending moments of the middle surface. Bilinear shape functions of local coordinates were used as approximating expressions for both force and displacement unknowns. The dimensions of the flexibility matrix of the four-node discretization element were found to be 36×36. The solution of benchmark problem of analyzing a truncated ellipsoid of revolution loaded with internal pressure showed sufficient accuracy in calculating the strength parameters of the studied shell.

Keywords: four-node discretization element, stress-strain state, flexibility matrix

Yuriy V. Klochkov, Doctor of Technical Sciences, Professor, Head of the Department of Higher Mathematics, Electric Power and Energy Faculty, Volgograd State Agrarian University, 26 Universitetskii Prospekt, Volgograd, 400002, Russian Federation; ORCID: 0000-0002-1027-1811, Scopus ID: 57170472500, eLIBRARY SPIN-code: 9436-3693; klotchkov@bk.ru

Valeriya A. Pshenichkina, Doctor of Technical Sciences, Professor, Head of the Department of Building Structures, Foundations and Reliability of Structures, Faculty of Construction and Housing and Communal Services, Volgograd State Technical University, 28 Leninskii Prospekt, Volgograd, 400005, Russian Federation; ORCID: 0000-0001-9148-2815, Scopus ID: 57189646401, eLIBRARY SPIN: 3399-0668; vap_hm@list.ru

Anatoliy P. Nikolaev, Doctor of Technical Sciences, Professor of the Department of Mechanics, Faculty of Engineering and Technology, Volgograd State Agrarian University, 26 Universitetskii Prospekt, Volgograd, 400002, Russian Federation; ORCID: 0000-0002-7098-5998, Scopus ID: 7202396806, eLIBRARY SPIN-code: 2653-5484; anpetr40@yandex.ru

Olga V. Vakhnina, Candidate of Technical Sciences, Associate Professor of the Department of Higher Mathematics, Electric Power and Energy Faculty, Volgograd State Agrarian University, 26 Universitetskii Prospekt, Volgograd, 400002, Russian Federation; ORCID: 0000-0001-9234-7287, Scopus ID: 55235780600, eLIBRARY SPIN-code: 3593-0159; ovahnina@bk.ru

Mikhail Yu. Klochkov, postgraduate student, Department of Building Structures, Foundations and Reliability of Structures, Faculty of Construction and Housing and Communal Services, Volgograd State Technical University, 28 Leninskii Prospekt, Volgograd, 400005, Russian Federation; ORCID: 0000-0001-6751-4629, Scopus ID: 57215535887, eLIBRARY SPIN-code: 2767-3955; m.klo4koff@yandex.ru

Четырехугольный конечный элемент в смешанной формулировке МКЭ для расчета тонких оболочек вращения

Ю.В. Клочков[1], В.А. Пшеничкина[2], А.П. Николаев[1], О.В. Вахнина[1], М.Ю. Клочков[2]

[1]*Волгоградский государственный аграрный университет, Волгоград, Российская Федерация*
[2]*Волгоградский государственный технический университет, Волгоград, Российская Федерация*
klotchkov@bk.ru

История статьи
Поступила в редакцию: 15 ноября 2022 г.
Доработана: 20 февраля 2023 г.
Принята к публикации: 24 февраля 2023 г.

Для цитирования
Клочков Ю.В., Пшеничкина В.А., Николаев А.П., Вахнина О.В., Клочков М.Ю. Четырехугольный конечный элемент в смешанной формулировке МКЭ для расчета тонких оболочек вращения // Строительная механика инженерных конструкций и сооружений. 2023. Т. 19. № 1. С. 64–72. http://doi.org/10.22363/1815-5235-2023-19-1-64-72

Аннотация. Цель исследования – разработка алгоритма конечно-элементного расчета тонких оболочек вращения на основе смешанной формулировки метода конечных элементов в двумерной постановке при использовании в качестве элемента дискретизации четырехугольного фрагмента срединной поверхности. Искомыми узловыми неизвестными были выбраны продольные усилия и моменты, а также компоненты вектора перемещения. Количество искомых неизвестных в каждом из узлов четырехузлового элемента дискретизации достигает девяти: шесть силовых и три кинематических искомых величин. Для получения матрицы податливости и столбца узловых усилий использовался модифицированный функционал Рейсснера, в котором полная удельная работа напряжений представлена удельной работой мембранных усилий и изгибающих моментов срединной поверхности на ее деформациях и искривлениях, а удельная дополнительная работа определена удельной работой мембранных усилий и изгибающих моментов срединной поверхности. В качестве аппроксимирующих выражений и для силовых, и для кинематических искомых неизвестных использовались билинейные функции формы локальных координат. Размерность матрицы податливости четырехузлового элемента дискретизации составила 36×36. Решение тестовой задачи по анализу напряженно-деформированного состояния усеченного эллипсоида вращения, загруженного внутренним давлением, показало достаточную для инженерной практики точность вычислений прочностных параметров исследуемой оболочечной конструкции.

Ключевые слова: четырехузловой элемент дискретизации, напряженно-деформированное состояние, матрица податливости

Introduction

Finite element analysis of thin shells based on the displacement method (when the unknown nodal variables are displacements and their partial derivatives) has been developed quite well and is widely used today in various software suites. In [1], FEM is presented as an alternative to the finite difference method with justification of its advantages. It is widely used in the calculations of beams and frame structures [2], as well as multi-

Клочков Юрий Васильевич, доктор технических наук, профессор, заведующий кафедрой высшей математики, электроэнергетический факультет, Волгоградский государственный аграрный университет, Российская Федерация, 400002, Волгоград, Университетский пр-кт, д. 26; ORCID: 0000-0002-1027-1811, Scopus ID: 57170472500, eLIBRARY SPIN-код: 9436-3693; klotchkov@bk.ru

Пшеничкина Валерия Александровна, доктор технических наук, профессор, заведующая кафедрой «Строительные конструкции, основания и надежность сооружений», факультет строительства и жилищно-коммунального хозяйства, Волгоградский государственный технический университет, Российская Федерация, 400005, Волгоград, пр-кт Ленина, д. 28; ORCID: 0000-0001-9148-2815, Scopus ID: 57189646401, eLIBRARY SPIN-код: 3399-0668; vap_hm@list.ru

Николаев Анатолий Петрович, доктор технических наук, профессор кафедры механики, инженерно-технологический факультет, Волгоградский государственный аграрный университет, Российская Федерация, 400002, Волгоград, Университетский пр-кт, д. 26; ORCID: 0000-0002-7098-5998, Scopus ID: 7202396806, eLIBRARY SPIN-код: 2653-5484; anpetr40@yandex.ru

Вахнина Ольга Владимировна, кандидат технических наук, доцент кафедры высшей математики, электроэнергетический факультет, Волгоградский государственный аграрный университет, Российская Федерация, 400002, Волгоград, Университетский пр-кт, д. 26; ORCID: 0000-0001-9234-7287, Scopus ID: 55235780600, eLIBRARY SPIN-код: 3593-0159; ovahnina@bk.ru

Клочков Михаил Юрьевич, аспирант, кафедра «Строительные конструкции, основания и надежность сооружений», факультет строительства и жилищно-коммунального хозяйства, Волгоградский государственный технический университет, Российская Федерация, 400005, Волгоград, пр-кт Ленина, д. 28; ORCID: 0000-0001-6751-4629, Scopus ID: 57215535887, eLIBRARY SPIN-код: 2767-3955; m.klo4koff@yandex.ru

layer plates and shells [3; 4], and in the calculation of three-dimensional structures and thick slabs [5; 6]. FEM was widely used in the formulation of the displacement method in the calculation of thin shells under elastic and elastoplastic deformation [7–11]. This method is also used in the analysis of the nonlinear deformation of plates and shells [12–15]. FEM is used in the formulation of the displacement method and in cases of large deformations during loading of plates and shells [16–18], as well as in shell stability calculations [19; 20]. In engineering stability problems, a mixed formulation based on the predictor-corrector scheme was proposed [21; 22]. To reach the appropriate level of accuracy for computing the unknown values, it is necessary to use the approximating expressions of class $C^{(2)}$, since the Cauchy relations for thin shells [23; 24] contain second order partial derivatives of the normal displacement vector. When using the mixed FEM (when the unknown nodal variables are displacements, axial forces and moments), approximating the unknowns with functions of classes $C^{(0)}$ and $C^{(1)}$ is sufficient. A major advantage of using the mixed FEM is the ability to compute stresses and deformations at an element node in terms of the evaluated unknowns of the element at this specific node. In contrast, to determine nodal stresses, FEM based on the displacement method requires calculating the unknowns at the adjacent nodes, which increases the computational error. In this regard, the most relevant problem now is the development of algorithms for linear and non-linear analysis of thin shells with the mixed FEM using curvilinear coordinates.

Methods

The Reissner functional is considered in the following definition [25; 26]:

$$\Phi_R = \int_V \underset{1\times3}{\{\sigma\}^T} \underset{3\times1}{\left\{\varepsilon^{\zeta}\right\}} dV - \frac{1}{2}\int_V \underset{1\times3}{\{\sigma\}^T} \underset{3\times3}{\left[C_{\varepsilon}\right]} \underset{3\times1}{\{\sigma\}} dV - \frac{1}{2}\int_F \underset{1\times3}{\{U\}^T} \underset{3\times1}{\{P\}} dF, \tag{1}$$

where $\{\sigma\}^T = \{\sigma_{11}\ \sigma_{22}\ \sigma_{12}\}$, $\left\{\varepsilon^{\zeta}\right\}^T = \left\{\varepsilon^{\zeta}_{11}\ \varepsilon^{\zeta}_{22}\ \varepsilon^{\zeta}_{12}\right\}$ are the stresses and deformations at a point in the shell, which is located at vertical distance ζ from the corresponding point of the middle surface; matrix $\left[C_{\varepsilon}\right]$ represents the transformation matrix from vector $\left\{\varepsilon^{\zeta}\right\}$ to vector $\{\sigma\}$, which is composed based on the Hooke's law for thin shells [23; 24]; $\{U\}^T = \{uvw\}$ is the row vector of displacement components of the middle surface point; $\{P\}$ is the external load vector.

Stresses $\{\sigma\}$ in functional (1) are expressed in terms of the forces of the middle surface [23; 24]:

$$\sigma_{11} = \frac{N_{11}}{h} + \frac{\zeta M_{11}}{I}; \quad \sigma_{22} = \frac{N_{22}}{h} + \frac{\zeta M_{22}}{I}; \quad \sigma_{12} = \frac{N_{12}}{h} + \frac{\zeta M_{12}}{I}, \tag{2}$$

where $I = \frac{h^3}{12}$ is the moment of inertia of the cross-section; h is the height of the cross-section.

Deformations of an arbitrary layer of the shell are determined in terms of membrane and bending strains by relations [23; 24]:

$$\varepsilon^{\zeta}_{11} = \varepsilon_{11} + \zeta\aleph_{11}; \quad \varepsilon^{\zeta}_{22} = \varepsilon_{22} + \zeta\aleph_{22}; \quad \varepsilon^{\zeta}_{12} = \varepsilon_{12} + 2\zeta\aleph_{12}. \tag{3}$$

Physical and geometric expressions (2) and (3) may be represented in matrix form:

$$\underset{3\times1}{\{\sigma\}} = \underset{3\times6}{\left[\Gamma_{\sigma}\right]} \underset{6\times1}{\{S_0\}}; \quad \underset{3\times1}{\left\{\varepsilon^{\zeta}\right\}} = \underset{3\times6}{\left[\Gamma_{\varepsilon}\right]} \underset{6\times1}{\{\varepsilon_0\}}, \tag{4}$$

where $\underset{1\times 6}{\{S_0\}^T} = \{N_{11}\ N_{22}\ N_{12}\ M_{11}\ M_{22}\ M_{12}\}$; $\underset{1\times 6}{\{\varepsilon_0\}^T} = \{\varepsilon_{11}\ \varepsilon_{22}\ \varepsilon_{12}\ \aleph_{11}\ \aleph_{22}\ \aleph_{12}\}$;

$$\underset{3\times 6}{[\Gamma_\sigma]} = \begin{bmatrix} \frac{1}{h} & 0 & 0 & \frac{\zeta}{I} & 0 & 0 \\ 0 & \frac{1}{h} & 0 & 0 & \frac{\zeta}{I} & 0 \\ 0 & 0 & \frac{1}{h} & 0 & 0 & \frac{\zeta}{I} \end{bmatrix}; \quad \underset{3\times 6}{[\Gamma_\varepsilon]} = \begin{bmatrix} 1 & 0 & 0 & \zeta & 0 & 0 \\ 0 & 1 & 0 & 0 & \zeta & 0 \\ 0 & 0 & 1 & 0 & 0 & 2\zeta \end{bmatrix}.$$

Membrane and bending strains of the middle surface are defined by expressions [27]:

$$\varepsilon_{\alpha\beta} = \frac{1}{2}\left(\vec{a}_\alpha^0 \vec{v}_{,\beta} + \vec{a}_\beta^0 \vec{v}_{,\alpha}\right); \quad \aleph_{\alpha\beta} = \frac{1}{2}\left(\vec{a}_{,\alpha}^0 \vec{v}_{,\beta} + \vec{a}_{,\beta}^0 \vec{v}_{,\alpha} + \vec{a}_\alpha^0 \vec{v}_{,\beta}^n + \vec{a}_\beta^0 \vec{v}_{,\alpha}^n\right), \tag{5}$$

where $\vec{a}_\alpha^0$ are the basis vectors of a middle surface point; $\vec{v}$ is the displacement vector of the middle surface point; $\vec{v}^n = \vec{a} - \vec{a}^0$ is the difference vector of normal lines of the middle surface point in the deformed and undeformed states.

Relationships (5) may be expressed in matrix form:

$$\underset{6\times 1}{\{\varepsilon_0\}} = \underset{6\times 3}{[L]}\underset{3\times 1}{\{U\}}, \tag{6}$$

where $\underset{6\times 3}{[L]}$ is the differentiation and algebraic expressions matrix.

Moments $M_{\alpha\beta}$ and forces $N_{\alpha\beta}$ at a point on the middle surface, which are contained in (2), may be expressed in terms of the values of these force unknowns at the nodes of the quadrilateral element using approximating bilinear functions with the following matrix product:

$$\underset{6\times 1}{\{S_0\}} = \underset{6\times 24}{[H]}\underset{24\times 1}{\{S_y\}}, \tag{7}$$

where $\underset{1\times 24}{\{S_y\}^T} = \{N_{11}^i\ N_{11}^j\ N_{11}^k\ N_{11}^l\ N_{22}^i \dots N_{22}^l\ N_{12}^i \dots N_{12}^l\ M_{11}^i \dots M_{11}^l\ M_{22}^i \dots M_{22}^l\ M_{12}^i \dots M_{12}^l\}$;

$$\underset{6\times 24}{[H]} = \begin{bmatrix} \underset{1\times 4}{\{\varphi\}^T} & & & & & \\ & \underset{1\times 4}{\{\varphi\}^T} & & & & \\ & & \underset{1\times 4}{\{\varphi\}^T} & & & \\ & & & \underset{1\times 4}{\{\varphi\}^T} & & \\ & & & & \underset{1\times 4}{\{\varphi\}^T} & \\ & & & & & \underset{1\times 4}{\{\varphi\}^T} \end{bmatrix};$$

$\underset{1\times 4}{\{\varphi\}^T} = \{\varphi_1\ \varphi_2\ \varphi_3\ \varphi_4\}$ are the bilinear functions of local coordinates $-1 \le \xi, \eta \le 1$ of the quadrilateral finite element [27].

Deformations at a middle surface point (6) may expressed using bilinear functions φ as the following matrix product:

$$\underset{6\times1}{\{\varepsilon_0\}} = \underset{6\times3}{[L]}\underset{3\times12}{[A]}\underset{12\times1}{\{U_y\}} = \underset{6\times12}{[B]}\underset{12\times1}{\{U_y\}}, \tag{8}$$

where $\underset{3\times12}{[A]} = \begin{bmatrix} \{\varphi\}^T & \{0\} & \{0\} \\ \{0\} & \{\varphi\}^T & \{0\} \\ \{0\} & \{0\} & \{\varphi\}^T \end{bmatrix}$; $\underset{1\times12}{\{U_y\}^T} = \left\{\{u_y\}^T \{v_y\}^T \{w_y\}^T\right\}$; $\underset{1\times4}{\{q_y\}^T} = \left\{q^i\ q^j\ q^k\ q^l\right\}$; q represents tangential u, v or normal w displacement vector component.

Considering (4), (6), (7) and (8), functional (1) may be represented as

$$\Phi_R = \underset{1\times24}{\{S_y\}^T} \iint_F \underset{24\times6}{[H]^T} \left[\int_{-\frac{h}{2}}^{\frac{h}{2}} \underset{6\times3}{[\Gamma_\sigma]^T} \underset{3\times6}{[\Gamma_\varepsilon]} d\zeta \right] \underset{6\times12}{[B]} dF \underset{12\times1}{\{U_y\}} -$$

$$-\frac{1}{2}\underset{1\times24}{\{S_y\}^T} \iint_F \underset{24\times6}{[H]^T} \left[\int_{-\frac{h}{2}}^{\frac{h}{2}} \underset{6\times3}{[\Gamma_\sigma]^T} \underset{3\times3}{[C_\varepsilon]} \underset{3\times6}{[\Gamma_\sigma]} d\zeta \right] \underset{6\times24}{[H]} dF \underset{24\times1}{\{S_y\}} - \frac{1}{2}\underset{1\times12}{\{U_y\}^T} \iint_F \underset{12\times3}{[A]^T} \underset{3\times1}{\{P\}} dF. \tag{9}$$

By minimizing functional (9) with respect to $\{S_y\}^T$, the following relation can be obtained:

$$\partial\Phi_R \big/ \partial\{S_y\}^T \equiv \underset{24\times12}{[Q]}\underset{12\times1}{\{U_y\}} - \underset{12\times24}{[Y]}\underset{24\times1}{\{S_y\}} = 0, \tag{10}$$

where $\underset{24\times12}{[Q]} = \iint_F \underset{24\times6}{[H]^T} \left[\int_{-\frac{h}{2}}^{\frac{h}{2}} \underset{6\times3}{[\Gamma_\sigma]^T} \underset{3\times6}{[\Gamma_\varepsilon]} d\zeta \right] \underset{6\times12}{[B]} dF$; $\underset{12\times24}{[Y]} = \iint_F \underset{24\times6}{[H]^T} \left[\int_{-\frac{h}{2}}^{\frac{h}{2}} \underset{6\times3}{[\Gamma_\sigma]^T} \underset{3\times3}{[C_\varepsilon]} \underset{3\times6}{[\Gamma_\sigma]} d\zeta \right] \underset{6\times24}{[H]} dF.$

In order to minimize functional (7) with respect to unknown nodal displacements $\{U_y\}$, equation (9) needs to be represented in the following form:

$$\underset{1\times12}{\{U_y\}^T} \iint_F \underset{12\times6}{[B]^T} \left[\int_{-\frac{h}{2}}^{\frac{h}{2}} \underset{6\times3}{[\Gamma_\varepsilon]^T} \underset{3\times6}{[\Gamma_\sigma]} d\zeta \right] \underset{6\times24}{[H]} dF \underset{24\times1}{\{S_y\}} -$$

$$-\frac{1}{2}\underset{1\times24}{\{S_y\}^T} \iint_F \underset{24\times6}{[H]^T} \left[\int_{-\frac{h}{2}}^{\frac{h}{2}} \underset{6\times3}{[\Gamma_\sigma]^T} \underset{3\times3}{[C_\varepsilon]} \underset{3\times6}{[\Gamma_\sigma]} d\zeta \right] \underset{6\times24}{[H]} dF \underset{24\times1}{\{S_y\}} - \frac{1}{2}\underset{1\times12}{\{U_y\}^T} \iint_F \underset{12\times3}{[A]^T} \underset{3\times1}{\{P\}} dF. \tag{11}$$

Minimizing (11) with respect to $\{U_y\}^T$ yields the following matrix expression:

$$\partial \Phi_R \Big/ \partial \{U_y\}^T = \underset{12\times 24}{[Q]}^T \underset{24\times 1}{\{S_y\}} - \underset{12\times 1}{\{f_y\}} = 0. \tag{12}$$

By rearranging (10) and considering (12), it is possible to obtain the flexibility matrix and the nodal forces vector for the quadrilateral element in the following form:

$$\underset{36\times 36}{\begin{bmatrix} -\underset{24\times 24}{[Y]} & \underset{24\times 12}{[Q]} \\ \underset{12\times 24}{[Q]^T} & \underset{12\times 12}{[0]} \end{bmatrix}} \underset{36\times 1}{\begin{Bmatrix} \underset{24\times 1}{\{S_y\}} \\ \underset{12\times 1}{\{U_y\}} \end{Bmatrix}} = \underset{36\times 1}{\begin{Bmatrix} \underset{24\times 1}{\{0\}} \\ \underset{12\times 1}{\{f\}} \end{Bmatrix}}. \tag{13}$$

Thus, the dimension of the flexibility matrix of the quadrilateral element is 36×36, and the nodal unknowns vector contains 24 force and 12 kinematic factors, which are axial forces $N_{\alpha\beta}$ and moments $M_{\alpha\beta}$ and displacement components of a nodal point of the middle surface.

Construction of the general flexibility matrix and nodal forces vector of the entire shell is conducted using the index matrix, which reflects the boundary conditions of the shell [28].

Results and discussion

Calculation example. In order to verify the developed algorithm, a truncated ellipsoid of revolution, which is illustrated in Figure, was analyzed.

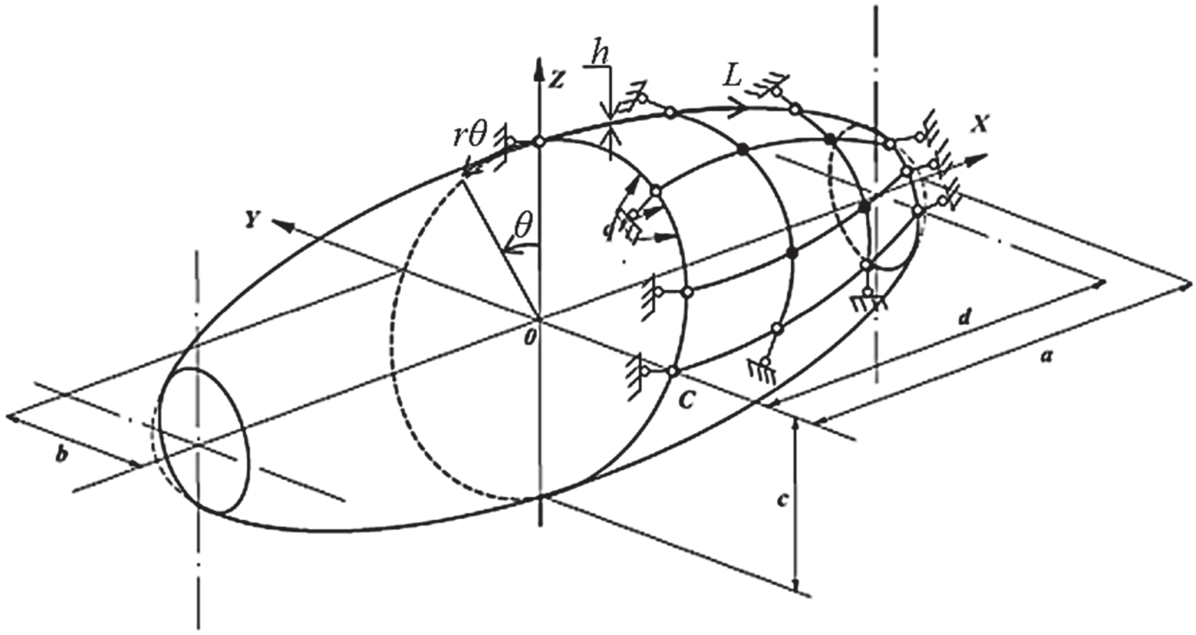

Truncated ellipsoid of revolution

The following initial data was adopted: ellipsoid shape parameters $a = 1.3$ m; $b = c = 0.9$ m; shell thickness $h = 0.02$ m; modulus of elasticity $E = 2\cdot 10^5$ MPa; Poisson's ratio $\nu = 0.3$; internal pressure $q = 5$ MPa. Only 1/8 of the shell was analyzed due to ellipsoid having planes of symmetry. The results of the analysis are presented in Table, in which the numerical values of normal stresses of the middle surface at the support ($x = 0.0$ m) and end ($x = 1.2$ m) sections of the ellipsoid with different finite element grid are given.

The results in Table imply that refining the grid leads to stable convergence of the computational process. However, convergence stability is a necessary, but not sufficient condition for the efficacy of the algorithm in regards to the real physical distribution of stress in the shell.

To evaluate the objectiveness of the results, let us compute meridional stress at the support and end sections. The meridional stress at the support section can be obtained from the following equilibrium equation:

$$\sigma_{11}\big|_{x=0} = \frac{q}{h2\pi R_0}\left(\pi R_0^2 - \pi R_k^2\right), \tag{14}$$

where R_0, R_k are the radii of revolution of the ellipsoid at the support and the end sections respectively, besides $R_0 = b = 0.9$ m; $R_k = \frac{b}{a}\sqrt{a^2 - x_k^2} = \frac{0.9}{1.3}\sqrt{1.3^2 - 1.2^2} = 0.346$ m.

Values of normal stresses in the middle surface of the ellipsoid

Section	Stress, MPa	Node grid					Analytical solution according to the Laplace equation
		41×41	61×61	81×81	101×101	121×121	
Support, $x = 0.0$ m	σ_{11}	95.93	95.89	95.88	95.87	95.87	95.86
	σ_{22}	179.03	179.04	179.05	179.05	179.05	179.06
End, $x = 1.2$ m	σ_{11}	0.916	0.449	0.270	0.182	0.133	0.00
	σ_{22}	167.75	168.45	168.78	168.96	169.06	167.82

By substituting the initial data into (14), it is possible to obtain the following value of meridional stress at the support section: $\sigma_{11}\big|_{x=0} = \frac{5}{0.02\cdot 2\pi\cdot 0.9}\left(\pi 0.9^2 - \pi 0.346^2\right) = 95.86$ MPa.

The meridional stress at the end section must be zero, since the right end of the shell is not loaded: $\sigma_{11}\big|_{x=1.2} = 0.00$ MPa.

Circumferential stress σ_{22} of the middle surface of the ellipsoid at the support and end sections may be expressed using the Laplace equation:

$$\frac{\sigma_{11}}{R_1} + \frac{\sigma_{22}}{R_2} = \frac{q}{h}. \tag{15}$$

Radii of curvature R_1 and R_2 in (15) are defined by

$$R_1 = -1\Big/\left(x_{,S}^3 r_{,xx}\right); \quad R_2 = 1\Big/\left(r/x_{,S}\right), \tag{16}$$

where $r = (b/a)\sqrt{a^2 - x^2}$ is the radius of revolution of the ellipsoid, $r_{,xx}$ is the second order derivative of the radius of revolution; $x_{,S} = 1\Big/\sqrt{1+\left(r_{,x}\right)^2}$.

Thus, it is possible to obtain the analytical value of circumferential stress at the support and end sections of the ellipsoid from (15):

$$\sigma_{22} = \left(\frac{q}{h} - \frac{\sigma_{11}}{R_1}\right)R_2. \tag{17}$$

Substituting the corresponding initial data into (17) yields the values of the desired stresses: $\sigma_{22}\big|_{x=0} = 179.06$ MPa; $\sigma_{22}\big|_{x=1.2} = 167.82$ MPa.

Conclusion

By comparing the analytical values of meridional stress σ_{11} and circumferential stress σ_{22} computed with equations (14)–(17) and the values obtained via the developed algorithm, it can be concluded that the adequate level of accuracy of the finite element analysis has been reached, as the minimum computational error does not exceed 1%. The developed algorithm may be recommended for application in engineering practice for the analysis of thin shells.

References

1. Bate K.-Yu. *Finite element methods.* Moscow: Fizmatlit Publ.; 2010. (In Russ.)

2. Lalin V., Rybakov V., Sergey A. The finite elements for design of frame of thin-walled beams. *Applied Mechanics and Materials.* 2014;578–579:858–863. https://doi.org/10.4028/www.scientific.net/amm.578-579.858

3. Agapov V. The Family of multilayered finite elements for the analysis of plates and shells of variable thickness. *E3S Web of Conferences. 2018 Topical Problems of Architecture, Civil Engineering and Environmental Economics, TPACEE 2018.* 2019. https://doi.org/10.1051/e3sconf/20199102013

4. Chernysheva N., Rozin L. Modified finite element analysis for exterior boundary problems in infinite medium. In V. Murgul (Ed.), *MATEC Web of Conferences.* 2016. https://doi.org/10.1051/matecconf/20165301042

5. Yakupov S.N., Kiyamov H.G., Yakupov N.M. Modeling a synthesized element of complex geometry based upon three-dimensional and two-dimensional finite elements. *Lobachevskii Journal of Mathematics.* 2021;42(9):2263–2271.

6. Tyukalov Yu.Ya. Quadrilateral finite element for thin and thick plates. *Construction of Unique Buildings and Structures.* 2021;5(98):9802. https://doi.org/10.4123/CUBS.98.2

7. Yamashita H., Valkeapää A.I., Jayakumar P., Sugiyama H. Continuum mechanics based bilinear shear deformable shell element using absolute nodal coordinate formulation. *Journal of Computational and Nonlinear Dynamics.* 2015;10(5):051012. https://doi.org/10.1115/1.4028657

8. Klochkov Y.V., Vakhnina O.V., Sobolevskaya T.A., Gureeva N.A., Klochkov M.Y. Calculation of an ellipsoid-shaped shell based on a consistent triangular discretization element with an in-variant interpolation procedure. *Journal of Machinery Manufacture and Reliability*. 2022;51(3):216–229. https://doi.org/10.3103/S1052618822030074

9. Klochkov Yu., Nikolaev A., Vakhnina O., Sobolevskaya T., Klochkov M. Physically nonlinear shell deformation based on three-dimensional finite elements. *Magazine of Civil Engineering.* 2022;5(113):11314. https://doi.org/10.34910/MCE.113.14

10. Klochkov Y.V., Nikolaev A.P., Vakhnina O.V., Sobolevskaya T.A., Klochkov M.Y. Variable formation plasticity matrices of a three-dimensional body when implementing a step loading procedure. *Journal of Physics: Conference Series. 5. V International Scientific and Technical Conference "Mechanical Science and Technology Update" (MSTU 2021).* 2021. https://doi.org/10.1088/1742-6596/1901/1/012118

11. Klochkov Yu.V., Vakhnina O.V., Sobolevskaya T.A., Klochkov M.Yu. Algorithm of finite elemental SSS analysis of thin-walled technosphere objects based on a triangular discretion element with elastic-plastic deformation. *Journal of Physics: Conference Series. International Conference on IT in Business and Industry (ITBI 2021).* 2021. https://doi.org/10.1088/1742-6596/2032/1/012028

12. Leonetti L., Magisano D., Madeo A., Garcea G., Kiendl J., Reali A. A simplified Kirchhoff – Love large deformation model for elastic shells and its effective isogeometric formulation. *Computer Methods in Applied Mechanics and Engineering.* 2019;354:369–396. https://doi.org/10.1016/j.cma.2019.05.025

13. Neto M.A., Amaro A., Roseiro L., Cirne J., Leal R. Finite element method for plates/shells. *Engineering Computation of Structures: The Finite Element Method.* Cham: Springer; 2015. p. 195–232. https://doi.org/10.1007/978-3-319-17710-6_6

14. Sultanov L.U. Analysis of finite elasto-plastic strains: integration algorithm and numerical examples. *Lobachevskii Journal of Mathematics*. 2018;39(9):1478–1483.

15. Serazutdinov M.N., Ubaydulloyev M.N. The method of calculating inelastic elements of rod structures under loading, unloading and reloading regimes. *Journal of Physics: Conference Series.* 2019. https://doi.org/10.1088/1742-6596/1158/4/042014

16. Garcea G., Liguori F.S., Leonetti L., Magisano D., Madeo A. Accurate and efficient a posteriori account of geometrical imperfections in Koiter finite element analysis. *International Journal for Numerical Methods in Engineering.* 2017;112(9):1154–1174.

17. Hanslo P., Larson Mats G., Larson F. Tangential differential calculus and the finite element modeling of a large deformation elastic membrane problem. *Computational Mechanics.* 2015;56(1):87–95.

18. Ren H. Fast and robust full-quadrature triangular elements for thin plates/shells, with large deformations and large rotations. *Journal of Computational and Nonlinear Dynamics.* 2015;10(5):051018. https://doi.org/10.1115/1.4030212

19. Kositsyn S.B., Akulich V.Yu. Numerical analysis of the stability of a cylindrical shell interacting with an inhomogeneous surrounding base. *Structural Mechanics of Engineering Constructions and Buildings.* 2021;17(6):608–616. (In Russ.) https://doi.org/10.22363/1815-5235-2021-17-6-608-616

20. Zheleznov L.P., Kabanov V.V., Boiko D.V. Nonlinear deformation and stability of discrete-reinforced elliptical cylindrical composite shells under torsion and internal pressure. *Russian Aeronautics.* 2018;61(2):175–182.

21. Lei Zh., Gillot F., Jezeguel. Developments of the mixed grid isogeometric Reissner – Mindlin shell: serendipity basis and modified reduced. *European Journal of Mechanics – A/Solids.* 2015;54:105–119. https://doi.org/10.1016/j.euromechsol.2015.06.010

22. Magisano D., Liang K., Garcea G., Leonetti L., Ruess M. An efficient mixed variation-al reduced-order model formulation for nonlinear analyses of elastic shells. *International Journal for Numerical Methods in Engineering.* 2018;113(4):634–655.

23. Novozhilov V.V. *Theory of thin shells.* St. Petersburg: St. Petersburg University Press; 2010. (In Russ.)

24. Chernykh K.F. *Nonlinear elasticity (theory and applications).* St. Petersburg; 2004. (In Russ.)

25. Rickards R.B. *The finite element method in the theory of shells and plates.* Riga: Zinatne Publ.; 1988. (In Russ.)

26. Gureeva N.A., Nikolaev A.P., Yushkin V.N. Comparative analysis of finite element formulations under plane loading of an elastic body. *Structural Mechanics of Engineering Constructions and Buildings.* 2020;16(2):139–145. https://doi.org/10.22363/1815-5235-2020-16-2-139-145 (In Russ.)

27. Nikolaev A.P., Klochkov Yu.V., Kiselev A.P., Gureeva N.A. *Vector interpolation of displacement fields in finite element calculations of shells.* Volgograd; 2012. (In Russ.)

28. Postnov V.A., Kharkhurim I.Ya. *Finite element method in calculations of ship structures.* Leningrad: Sudostroenie Publ.; 1974. (In Russ.)